LIGHT-ADJUSTABLE LENS

BY *Daniel M. Schwartz MD*

ABSTRACT

Purpose: First, to determine whether a silicone light-adjustable intraocular lens (IOL) can be fabricated and adjusted precisely with a light delivery device (LDD). Second, to determine the biocompatibility of an adjustable IOL and whether the lens can be adjusted precisely in vivo.

Methods: After fabrication of a light-adjustable silicone formulation, IOLs were made and tested in vitro for cytotoxicity, leaching, precision of adjustment, optical quality after adjustment, and mechanical properties. Light-adjustable IOLs were then tested in vivo for biocompatibility and precision of adjustment in a rabbit model. In collaboration with Zeiss-Meditec, a digital LDD was developed and tested to correct for higher-order aberrations in light-adjustable IOLs.

Results: The results establish that a biocompatible silicone IOL can be fabricated and adjusted using safe levels of light. There was no evidence of cytotoxicity or leaching. Testing of mechanical properties revealed no significant differences from commercial controls. Implantation of light-adjustable lenses in rabbits demonstrated excellent biocompatibility after 6 months, comparable to a commercially available IOL. In vivo spherical (hyperopic and myopic) adjustment in rabbits was achieved using an analog light delivery system. The digital light delivery system was tested and achieved correction of higher-order aberrations.

Conclusion: A silicone light-adjustable IOL and LDD have been developed to enable postoperative, noninvasive adjustment of lens power. The ability to correct higher-order aberrations in these materials has broad potential applicability for optimization of vision in patients undergoing cataract and refractive surgery.

Trans Am Ophthalmol Soc 2003;101:411-430

INTRODUCTION

With the advent of phacoemulsification and foldable intraocular lenses (IOLs), cataract surgery has become a highly evolved surgical procedure.[1] While the technical aspects of cataract surgery have become increasingly sophisticated, problems of precise IOL power selection remain unsolved. Specifically, calculations of IOL power are sometimes imprecise because of inaccurate preoperative measurements, postoperative astigmatism, or variability in position of the IOL.[2-13] With current methods of IOL power determination, the vast majority of patients see 20/40 or better without correction. A much smaller percentage achieve optimal vision without spectacle correction. Nearly all patients are within 2 diopters (D) of emmetropia. Of 298 emmetropic (<±0.5 D) patients undergoing phacoemulsification or extracapsular cataract surgery with posterior chamber lens placement, only 45% had an emmetropic refraction postoperatively despite the intention of the surgeon to achieve this result.[2] The remaining patients required spectacle correction for optimal distance vision. Ninety-four percent of patients in this group had a postoperative refractive error within 2 D of emmetropia. In a study of 1,473 patients, of which 884 (60%) underwent extracapsular surgery and 589 (40%) phacoemulsification, 1,429 patients (97%) were within 2 D of the intended refractive outcome.[3] Similarly, Wegener and coworkers[4] reported refractive outcomes of 950 patients undergoing cataract surgery, of which 441 (46%) were by extracapsular cataract extraction (ECCE) and 509 (54%) were by phacoemulsification. In this study, 855 patients (90%) were within 2 D of emmetropia postoperatively. In 1,320 cataract extractions on patients without ocular comorbidity, Murphy and coworkers[5] found that 858 (65%) had uncorrected visual acuity ≥20/40. In a comparison of visual function in 102 patients (all with ≤1.5 D of cylinder) implanted with a monofocal IOL in one eye and a multifocal IOL in the fellow eye, 93 (91%) achieved uncorrected vision of 20/40 or better, while only 31 (30%) achieved 20/20 or better without spectacle correction in the monofocal IOL-implanted eyes.[12] In the monofocal IOL group, 60 patients (59%) had best corrected vision of

From the University of California, San Francisco. This work is supported by grant 2R44EY012181-02 (Postoperative Adjustment of Intraocular Lens Power) from the National Eye Institute. The author is an inventor on a patent held by California Institute of Technology and the Regents of the University of California and is a stockholder and consultant for Calhoun Vision, Inc, Pasadena, Calif.

20/20 or better. Using partial coherence interferometry to obtain more accurate biometry (IOLMaster, Zeiss Humphrey Systems, Dublin, Calif), Connors and coworkers[10] found that postoperative spherical equivalent refractive error was within 0.5 D in 68 of 111 patients (61%) and within 1.0 D in 97 of 111 patients (87%). In a 2001 survey of cataract surgeons explanting foldable IOLs, the leading cause for removal among 3-piece silicone IOLs was incorrect IOL power.[13]

Irrespective of appropriate IOL power selection, uncorrected visual acuity may be reduced by preexisting astigmatism. In a series of 7,500 eyes undergoing cataract surgery, Hoffer[14] showed that 1,770 (23.6%) had ≥1.5 D of corneal astigmatism. A toric IOL with plate haptics is available from Staar Surgical (Monrovia, Calif) to correct >1.5 D of cylinder. The IOL comes in two toric powers (2.0 D, 3.5 D) and the axis must be precisely aligned at surgery. Other than surgical repositioning, there is no way to adjust the IOL's axis, which may shift postoperatively.[15,16] In a series of 130 eyes undergoing implantation of a toric IOL and followed for 3 months, 12 (9.2%) required secondary surgery to reposition the axis. In this study, 33 patients (25%) demonstrated significant axis shifts of >20°.[15] Furthermore, individualized correction of astigmatism is limited by unavailability of multiple toric powers. An additional problem with using preexisting astigmatic errors to gauge axis and power of a toric IOL is the unpredictable effect of the cataract wound on final refractive error. After the refractive effect of the cataract wound stabilizes, there can be a shift in both magnitude and axis of astigmatism, minimizing the corrective effect of a toric IOL. A means to postoperatively adjust (correct) astigmatic refractive errors *after* cataract surgery would be desirable.

Implantation of multifocal IOLs in which patients can potentially be spectacle-free for both near and distance has further increased the need for precise IOL power determination.[12,17-19] The Advanced Medical Optics (AMO, Santa Ana, Calif) Array multifocal IOL has five concentric zones of progressive aspheric lenses permitting simultaneous focusing at distance, near, and intermediate range. If the power calculation is correct for a multifocal IOL, patients potentially can achieve spectacle-free vision postoperatively. Patients implanted with multifocal IOLs often note glare at night, reduced contrast sensitivity, and mild limitation of near visual acuity.[17,18] These side effects of multifocality can be offset when patients achieve spectacle independence, which often remains elusive due to imprecise IOL power determination. Another limitation of multifocal IOLs is patient intolerance to multifocality. These patients sometimes require surgical explantation to relieve their symptoms.[13] More recently, multifocal IOLs have been implanted after clear lens extraction to treat high myopia and hyperopia.[20-22] This subset of patients who undergo surgery to reduce spectacle dependence are especially desirous of achieving emmetropia.

Clinical trials of phakic IOLs for correction of high myopia and hyperopia have increased the emphasis on precise IOL power determination.[23-26] Correction of high myopic refractive errors with excimer laser corneal surgery requires extensive ablation of corneal tissue, with resultant less predictable refractive outcomes and increased rates of glare and haloes. Using phakic IOLs to treat high myopia potentially provides better predictability and optical quality than corneal-based refractive surgery. Whether implanting anterior chamber angle–supported, anterior chamber iris–fixated, or posterior chamber sulcus–supported phakic IOLs, optimization of this refractive therapy remains limited by imprecision in IOL power selection. Other factors, such as biocompatibility and risk of intraocular surgery, will need to be addressed before phakic IOLs emerge as an alternative to corneal refractive surgery.

Eyes undergoing corneal refractive procedures (approximately 1.5 million per year in the United States) that subsequently develop cataracts are challenging with respect to IOL power determination. Corneal topographic alterations induced by refractive surgery reduce the accuracy of keratometric measurements, often leading to significant postoperative ametropia.[27-30] Recent studies of patients who have had corneal refractive surgery (photorefractive keratectomy, laser in situ keratomileusis, radial keratotomy) and then required subsequent cataract surgery frequently demonstrate hyperopic refractive "surprises" postoperatively. As the refractive surgery population ages and begins developing cataracts, appropriate selection of IOL power for these patients will become an increasingly challenging clinical problem. The ability to address this problem with an adjustable IOL would be desirable.

Previous investigators have recognized the need for an adjustable IOL.[31-37] Krasner[31] has patented a three-piece IOL with an inflatable diaphragm. Injection or removal of fluid from the flexible optic is used to postoperatively adjust IOL power. Only spherical corrections are achieved, and adjustment is an invasive procedure with attendant risks. Eggleston and Day[32,33] patented a mechanically adjustable IOL whose power is adjusted by rotation of the optic in a screw guide. The patent claims such adjustment could be made noninvasively if performed with magnets. O'Donnell[34,35] uses light energy to change the shape of an IOL in situ. This has the advantage of noninvasive adjustment. However, the precision of such methods of power change and their adaptability to currently used foldable materials are not clear from his patents.

An ideal adjustable IOL must meet the following criteria:

- Safe, noninvasive adjustment procedure performed postoperatively
- Stable, precise correction (within 0.25 D) of myopic, hyperopic, and astigmatic refractive errors
- Refractive error correction range ≥2.0 D
- Foldable for small-incision surgery
- Biocompatible

The author hypothesized that a light-adjustable IOL could be designed that met these design criteria. To prove this hypothesis and develop a light-adjustable IOL, a collaboration with scientists at California Institute of Technology was established. Taking advantage of silicone's low glass transition temperature and resultant facility with which silicone molecules can diffuse in a silicone polymer matrix at body temperature, we developed an adjustable silicone IOL whose power is adjusted using low levels of light energy (Light-Adjustable Lens, LAL).[38,39] The silicone formulation used in the LAL is based upon a silicone matrix system comprised of polymer, resin, crosslinker, and platinum catalyst. Formulated into the silicone matrix are a photoreactive macromer, photoinitiator, and UV absorbers. The UV absorbers are conjugated onto the silicone matrix. The photosensitive macromer system was designed to be compatible with the silicone matrix and insoluble in water to prevent leaching into the eye. It also was formulated to remain optically clear upon forming an interpenetrating network within the matrix upon irradiation with light at 365 nm.

Irradiation of the LAL with UV light (wavelength, 365 nm) causes the photosensitive macromers to polymerize and form silicone polymers in the irradiated region. For example, if a central optical zone is irradiated, macromers polymerize in that region alone. Following this polymerization, macromers in the peripheral, unirradiated portions of the IOL are highly concentrated relative to the central irradiated zone, where they have been depleted by the irradiation. This creates a thermodynamically unstable diffusion gradient, which is corrected over 12 to 15 hours as macromers diffuse toward the irradiated region to once again establish a uniform concentration throughout the matrix. As the macromers migrate centrally, this portion of the lens swells and refractive power increases (Figure 1) to correct hyperopia.

Once the appropriate power adjustment is achieved, the entire lens is irradiated to polymerize the remaining reactive macromer, thus preventing additional change in lens power. By irradiating the entire lens, macromer diffusion resulting from concentration gradient does not occur, and thus no change in lens power results. This second irradiation procedure is referred to as "lock-in." By controlling the irradiation dosage (ie, intensity and duration), beam intensity profile, and targeted area, changes in the radius of curvature are achieved, to either add or subtract spherical or cylindrical power (Figures 1 and 2).

To assess whether a LAL can be fabricated that would be useful in a clinical setting, a number of experiments were performed to establish feasibility. Any novel IOL material must be biocompatible. In the case of the LAL, there are really *two* IOLs being implanted: the nonadjusted LAL that contains unpolymerized macromer and the locked-in LAL in which macromer has been polymerized to silicone polymers. Biocompatibility was evaluated for both forms of the LAL. Because of the high physiochemical affinity of silicone macromers for the silicone matrix, it would not be anticipated that these macromers would leach out into the aqueous. Safety tests must establish the hydrolytic stability and photostability of the LAL. These test protocols not only establish the physical stability of the material but also quantitate the amount of leachable materials when incubated in saline under standard exposure conditions. A number of related in vitro tests are required to assess the mechanical properties of a novel IOL material.

In addition to biocompatibility, the adjustment of the LAL must be highly reproducible (within 0.25 D of the desired power) and optical quality must be maintained. Lock-in dosing must not significantly alter the adjusted power or the optical quality of the LAL. Therefore, it is necessary to determine whether a dose-response curve (nomogram) can be developed in which adjusted power varies as a function of treatment duration and intensity. Naturally, to be clinically useful, treatment duration and intensity must be constrained by what is safe and clinically practical. Thus, irradiations must not damage ocular tissues and should be performed within an approximate 2-minute time frame, commensurate with excimer laser treatments.

Once in vitro testing demonstrates feasibility of the LAL, a light delivery device (LDD) must be developed to treat patients. Initially, because treatments are performed on anesthetized rabbits, an operating microscope delivery system is desirable. Later, a slit lamp–based system would be preferred to use in an outpatient setting.

In designing the LAL, the best features of state-of-the art foldable IOLs were selected. These would include edge designs to minimize posterior capsule opacification (PCO). Haptics were selected that minimize LAL rotation, so that toric adjustments will not be subject to rotational alterations. In essence, the LAL was designed to be identical to current optimized foldable IOL designs, except for the capacity to adjust its power postoperatively.

In a series of in vitro and in vivo studies, we establish the feasibility of a silicone LAL. The fundamental properties underlying adjustability allow adaptation of the

technology to other foldable materials, such as acrylic. Furthermore, we demonstrate the versatility of light-adjustable materials to correct higher-order aberrations that would allow potential achievement of improved quality of vision.

METHODS

1. LIGHT-ADJUSTABLE INTRAOCULAR LENS

The LAL is a three-piece silicone lens with blue polymethyl methacrylate (PMMA) modified-C haptics, a 6.0-mm biconvex optic, and an overall length of 13.0 mm. Lenses in a range from 17 to 24 D have been designed. The LAL material was formulated to provide a UV cutoff at 10% transmission equals 385 nm.

In designing the LAL, the best features of state-of-the-art foldable IOLs were selected. The optic edge was designed with a square edge on the posterior surface and a round edge on the anterior surface to minimize PCO.[40,41] The modified-C haptic design with a 10° angle was selected to promote IOL stability in the capsular bag, minimizing the occurrence of LAL rotation that could offset toric adjustment.[42] In essence, the LAL is identical to current silicone IOLs, except for its capacity to adjust its power postoperatively.

2. LIGHT-ADJUSTABLE LENS FORMULATION

Silicone was selected for the adjustable lens technology because of its optical clarity, ability to be folded during insertion, and history of safe use in intraocular lenses. The silicone formulation used in the LAL is based upon a silicone matrix system composed of polymer, resin, crosslinker, and platinum catalyst. The silicone matrix material is supplied by NuSil (Carpinteria, Calif), an established supplier of medical-grade silicone. Formulated into the silicone matrix are a photoreactive silicone macromer, benzoin-based photoinitiator, and UV absorbers. The UV absorbers are conjugated onto the silicone matrix.

The silicone matrix material is supplied as two liquid components, which when mixed, form the lens matrix through a platinum-catalyzed hydrosilation reaction. Dispersed within the matrix are the low-molecular-weight silicone macromer molecules with photoreactive chain ends.

The benzoin-based photoinitiator was selected for its activity at 365 nm. The selection and concentrations of the UV absorber system and photoinitiator were optimized to allow for efficient photoinitiation at safe levels of UV irradiation and at the same time provide adequate UV protection for the retina in the pseudophakic eye. The photosensitive macromer system was designed to be compatible with the silicone matrix and insoluble in water to prevent leaching into the eye and to remain optically clear upon forming an interpenetrating network within the matrix upon irradiation with light at 365 nm.

3. LIGHT DELIVERY DEVICE

The LDD is used to deliver light of a selected wavelength (365 nm), spatial intensity profile, and diameter to produce a predictable change in the power of the LAL. The LDD is depicted in Figure 3.

The LDD consists of a UV light source, projection optics, and control interface installed on a standard slit lamp. The light source employed is a mercury (Hg) arc lamp delivered to projection optics through a liquid-filled light guide. The light source includes a narrow bandpass interference filter producing a beam with a center wavelength of 365 nm. An apodizing filter is included in the optical assembly that creates a specific beam-intensity profile (or pattern) projected onto the implanted lens.

The projection system is of a Kohler design, in which the source is imaged into the entrance pupil of the projection optics. This feature ensures that the field at the apodizing filter is sufficiently flat so that the optical density profile on the apodizing filter is accurately projected. The LDD is designed to guarantee alignment of the adjustment and photolocking beam with the LAL. The LDD projects an alignment reticle image to the surgeon's eye through a common optical path shared with the UV light projection optics. The reticle image and UV light profile are both parfocal and parcentral to within 50 µm. The reticle image is visualized through the microscope of a standard slit lamp, which serves as the mechanical support for the LDD. The line width of each reticle feature is 35 ± 5 µm in width, giving good visualization of the alignment target.

Ocular alignment is maintained by the patient viewing a fixation target that is parcentral to the delivery beam. The fixation target appears at infinity and subtends 0.25 degrees of arc. The fixation target has an adjustable intensity and is modulated to flash at a fixed frequency to hold the patient's attention.

The LDD is operated through a computer interface that controls the characteristics and initiation of the light beam delivery. A foot switch and keyboard are used to control the interface.

4. IRRADIATION SAFETY AT 365 nm

From a phototoxicity standpoint, the two most important ocular structures that would be affected by treatment of the LAL with 365-nm light are the cornea and the retina. Zuclich and Connolly[43] exposed rhesus monkey corneas to lasers operating in the 350- to 365-nm range and determined that corneal damage occurred following incident energy doses of between 60 and 70 J/cm^2 for pulsewidths ranging from 250 mseconds to 120 seconds. In addition,

irradiation dose studies performed on aphakic rhesus monkeys have shown that the retinal damage energy threshold is 5.4 J/cm^2 and 8.1 J/cm^2 for 350 nm and 380 nm radiation, respectively.[44] These data were reviewed with Dr David Sliney, Program Manager of the Laser/Optical Radiation Program at the US Army Center for Health Promotion and Preventive Medicine. Dr Sliney is widely published on the subject of the effects of UV radiation on the eye and serves as member, advisor, and chairman of numerous committees and institutions that are active in the establishment of safety standards for protection against nonionizing radiation.

Dr Sliney recommended in the current LDD design an upper limit corneal dose of 365 nm radiant energy on the order of 27 J/cm^2 and a maximum retinal dose of 2 J/cm^2 (after the beam passes through the UV blockers in the LAL) within any 24-hour period. Irradiation below these limits will not damage the cornea and retina or any other ocular tissue. Therefore, the development of adjustment and lock-in doses must meet these established safe limits.

IN VITRO TESTING

In vitro testing was conducted according to the International Organization for Standardization (ISO) guidelines as follows:

A. Cytotoxicity

Cytotoxicity of nonirradiated and irradiated silicone LALs was carried out in accordance with ISO 10993-5[45] using the ISO minimum essential medium (MEM) elution method. Triplicate extracts of each of the sample, negative control, reagent control, and positive controls were prepared. Each extract was placed onto separate confluent monolayers of L-929 mouse fibroblast cells and incubated at 37°C in 5% CO_2 for 48 hours. The monolayer was examined to determine any change in cell morphology microscopically (100×).

In addition, cytotoxicity tests of the individual photoactive components, ie, macromer and photoinitiator, were performed using the ISO MEM elution method. The macromer and photoinitiator were extracted individually in 0.9% NaCl irrigation solution using a ratio of 4 g:20 mL at 37°C for 24 hours. Following extraction, each vial was centrifuged and the supernatant was used for testing.

B. Hydrolytic Stability

The test samples (both irradiated and nonirradiated) in the form of rectangular slabs (0.8 cm × 1.8 cm) cut from 2-mm-thick cured film of LAL material, sham processed and ethylene oxide sterilized, were used. Test slabs were extracted in physiological saline (0.9% NaCl) at 37°C and 50°C for 72 hours, 30 days, and 90 days at a ratio of 1 g of material per 10 mL of saline. The test samples and/or saline extracts were analyzed at each of the three specified exposure periods by percent light transmission, refractive index, percent total extractables by exhaustive extraction, weight loss, physical damage, and leachable UV absorber, macromer, photoinitiator, and degradation products by high-pressure liquid chromatograph (HPLC) and gas chromatograph (GC) analysis. The lack of discoloration of test samples was verified at each exposure period by slit-lamp microscopic examination using a slit at an oblique-angle light.

C. Photostability

The test samples in the form of disks (6 mm in diameter) or rectangular slabs (0.8 cm × 2 cm × 2 mm), sham processed and ethylene oxide sterilized, were used. The disk samples were placed into individual quartz vials containing 0.9% saline in a ratio of one lens per 2 mL saline, sealed, and exposed to an accelerated UV-A (300 to 400 nm) light for a period of time calculated to simulate a 20-year intraocular exposure at 37°C. A second set of test samples was placed in an oven at 37ºC to serve as dark controls. At the end of exposure, the test slabs/disks and saline extracts were subjected to leachable components assay, weight loss determination, percent light transmission, and discoloration test. The results were compared to those of dark controls to ascertain that no significant deterioration had occurred.

D. Nd:YAG Laser Exposure Test

In order to determine the effects of Nd:YAG laser usage on LAL, the locked-in LALs were immersed in an optical cuvette containing 2 mL of physiological saline and subjected to Nd:YAG laser irradiation at a power setting of 5 mJ for 50 hits. The hits were focused on the posterior surface and distributed evenly over the central 3 mm optic zone of the LAL. The exposed lenses were evaluated for physical damage by light microscopy and scanning electron microscopy. Optical performance including back focal length and resolution was measured before and after Nd:YAG laser exposure. The saline surrounding the lenses during Nd:YAG laser exposure was tested for cytotoxicity by MEM elution method and for potential released substances by HPLC and GC analysis.

E. LAL Mechanical Property Assessment

The finished sterile LALs were subjected to standard lens mechanical tests (ISO 11979-3) for compression force, axial displacement in compression, optic decentration, optic tilt, angle of contact, compression force decay, dynamic fatigue durability, loop pull strength, surface and bulk homogeneity, and folding and injection testing.[46] The

acceptable limits established by the Food and Drug Administration (FDA) and ISO were used to verify that LAL performs comparably to established industry IOLs.

F. Optical Performance Testing

The optical performance of LALs, including the dioptric power change, resolution efficiency, modulation transfer function (MTF), and spectral transmittance, was evaluated in accordance with ISO standard test methods for IOLs (ISO/DIS 11979-2).[47] Each of the test methods is briefly described below:

Dioptric Power. Dioptric power of an intraocular lens can be determined by calculation from measured dimensions, back focal length (BFL), and line pair separation (LPS) by magnification. The optical bench illustrated in Figure 4 can be used for both BFL and LPS measurements.

Resolution Efficiency. The resolution limit of an IOL, expressed as a percentage of the diffraction-limited cut-off spatial frequency of an ideal lens having the same focal length, is determined using an optical bench with a US Air Force 1951 Resolution Target, diffusely illuminated by a monochromatic light source of 546 nm and an aperture of 3 mm. The finest pattern (group, element) for which both horizontal and vertical bars are resolved is recorded. The resolution efficiency (RE), expressed as a percentage of the cut-off spatial frequency, is calculated from the following equation:

$$RE = 100 \times 2^{[G + (E-1)/6]} \times (F\lambda)/(nd)$$

Where:
G = group of the pattern
E = element within the group of the pattern
F = focal length, in mm of the collimator
λ = wavelength of the light, in mm = 0.000546 mm
n = refractive index of the surrounding medium = 1 (air) or 1.33 (water)
d = aperture in mm = 3 mm

Modulation Transfer Function. The MTF is measured using monochromatic light (546 nm) with the IOL placed in a model eye in water at ambient temperature. The model eye is mounted on an optical bench making sure that the IOL is well aligned with the optical axis of the bench and focused to obtain maximum MTF at 100 mm^{-1} conforming to the requirements of ISO 9335.[48] The MTF value shall meet either of the two conditions: (1) greater than or equal to 0.43, or (2) greater than or equal to 70% of that calculated as maximum attainable for the LAL in question, but in any case greater than or equal to 0.28.

Spectral Transmittance. The spectral transmittance in the range of 300 nm to 1,200 nm is measured for the IOL with a dioptric power of 20 D or its equivalent (a flat piece of the IOL optic material having an average thickness equal to that of the central 3 mm of the 20 D IOL) using a UV-visible spectrophotometer.

G. *Power Adjustment and Lock-in Nomogram Development*
Nomogram Development.

An interferometer/irradiation system was developed in the laboratory to irradiate the LALs and measure precisely the power change following irradiation. A schematic of this system is displayed in Figure 5. Standard optical cells with PMMA "corneas" (Figure 6) were used to house LALs in water at 35°C. A slit lamp–based LDD emitting UV light at 365 nm was developed to treat the LALs clinically (Figure 3).

Apodizing filters were used to generate appropriate profiled beams to customize positive and negative corrections. The nomogram was developed by keeping the intensity of the treatment beam constant but varying the duration of treatment time between 0 and 210 seconds (dose within establish safe limits). Thirty LALs were irradiated at each time point (0, 30, 60, 75, 90, 105,120, 150, 180, 210 seconds). Following irradiation, LALs were kept in the wet cell at 35°C for 20 to 24 hours to allow the diffusion of macromer and an attendant shape change. The power was then measured using the interferometric and LPS methods.

*Effectiveness of Lock-in Procedure***.** For the power to be stable, the LAL must be locked in completely after adjustment to prevent power change due to potential polymerization of the residual unreacted macromer by ambient light. A solar simulator apparatus powered by a xenon arc lamp with filters to exclude light of wavelength less than 300 nm and an Air Mass 1 filter to simulate the sunlight spectrum at noon was used for this purpose. Locked-in LALs were placed in individual optical cuvettes in water and exposed in the solar simulator at an intensity of 0.3 mW/cm^2 at 37°C. Induced power changes were monitored using LPS and Fizeau interferometry. The following equation was used to calculate simulated in vivo exposure time.

$$T_2 = 365 \times T_1 \times [\ (I_2 / I_1) \times (24 / t)\ ]^{-1}$$

Where:

T_2 = in vitro test period (day)

T_1 = in vivo exposure time (year)

I_2 = in vitro intensity (mW/cm^2)

I_1 = in vivo UV-A radiation intensity = 0.3 mW/cm^2

t = daily exposure time to sunlight (hour) = 3

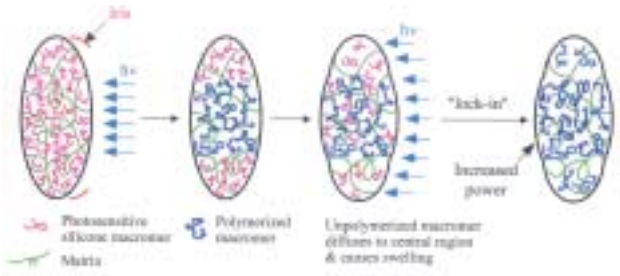

FIGURE 1

Correction of hyperopia. Silicone light-adjustable lens (LAL) is shown in cross section. A hyperopic correction is performed by irradiating the central portion of the LAL. This accomplishes a polymerization of photosensitive silicone macromers (red squiggles) that are embedded within the silicone matrix (green lines). Polymerization of the treated area is indicated by the thick blue lines. Polymerization does not change the LAL power (note same curvature of lens in second frame); however, it does create a concentration gradient between the peripheral, untreated portions of the LAL where macromer remains and the central, treated portion of the LAL, which is depleted of macromer. Over the next 12 to 15 hours, macromer diffuses down the gradient into the center of the LAL, causing it to swell. This increases its power. On the basis of the duration and power of exposure, differing amounts of hyperopia can be corrected. After the desired power change is confirmed (1 day after adjustment), the entire LAL is treated to polymerize remaining macromer. This locks in the power so that no further changes occur.

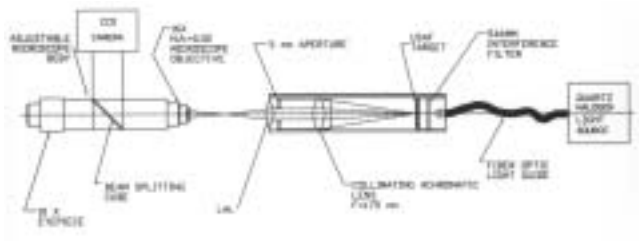

FIGURE 4

Optical bench for measuring intraocular lens (IOL) power. The optical bench consists of a US Air Force 1951 Resolution target back-illuminated by a lamp source spectrally filtered to 546 nm ± 10 nm. The illuminated target is placed in the focal plane of an achromatic collimator having a focal length of at least ten times that of the IOL under test. A 3-mm aperture is placed over the IOL, and the microscope (using a 16× objective with NA = 0.32) is focused at the back surface of the IOL. The microscope body is then adjusted to focus on the image of the target. The distance from the back surface of the IOL to the image is the back focal length (BFL). Determination of the paraxial dioptric power from the BFL is accomplished by calculating the distance from the back vertex of the IOL to the back principal plane of the IOL, calculating the contribution of the spherical aberration from standard ray trace procedures, and then adding these corrections to the BFL. In the case of line pair separation, the target has a measurable linear dimension, such as distance between two lines. The microscope has a reticle to measure the same linear dimension in the image.

Solar Exposure Studies. Because adjustment and lock-in of the LAL would ordinarily be performed 2 to 4 weeks postoperatively, during which time the LAL is UV light reactive, it is necessary to establish the safety margin of the LAL upon sunlight exposure before undergoing lock-in. Although patients are required to wear protective

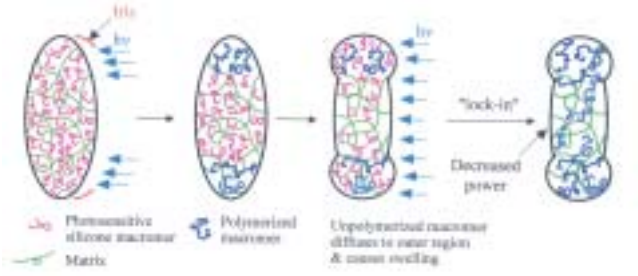

FIGURE 2

Correction of myopia. To treat myopia, the edges of the light-adjustable lens (LAL) are treated. Polymerization and consumption of macromer in the LAL periphery cause macromer to diffuse outward. This reduces the volume of macromer in the central portion of the lens, resulting in lens flattening, or reduction in power.

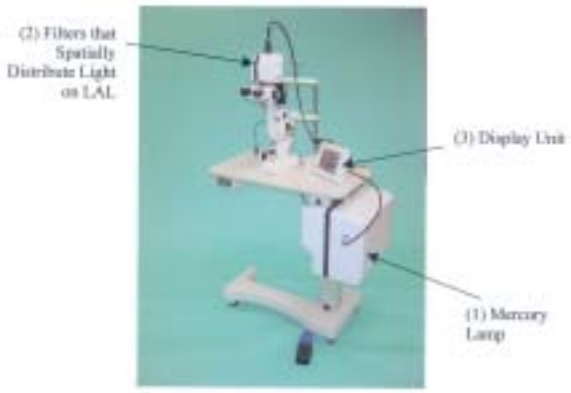

FIGURE 3

Analog light delivery device (LDD): A mercury lamp (1) provides output at irradiating wavelength of 365 nm. A profiled beam is generated by apodizing filters (2) to effect correction of hyperopia, myopia, and cylindrical errors. Refractive error and desired refractive outcome are entered on a touch-screen display unit (3).

sunglasses during the period before adjustment and lock-in treatments, they might forget to wear sunglasses, which may cause a premature and unpredictable photopolymerization of the macromer and resultant power change. Unirradiated 20-D LALs were placed in individual wet cells with filters to mimic the cornea transmission properties and exposed to sunlight in Pasadena, Calif, at noon in June to simulate the worst exposure condition encountered by patients without wearing sunglasses. LALs were exposed for 30, 60, and 120 minutes. Induced power changes were measured using Fizeau interferometry (Figure 5).

Stability and Predictability of LAL on the Shelf. The shelf-life stability of a group of finished sterile LALs stored for 4.5 months in ambient (indoor) light was evaluated. Lens dimensions (overall diameter and haptic angle), optical performance (BFL, resolution, and MTF), and power adjustment performance of the stored LALs were evaluated and compared to those freshly manufactured.

A set of 8 LALs stored for 4.5 months was irradiated in vitro with a dose of 1,200 mJ/cm^2. The final dioptric change of these aged LALs was compared to the dioptric response for a series of 12 freshly manufactured LALs irradiated under the same condition. The resolution efficiency data (ISO 11979-2, wet cell) and the MTF were also determined (ISO 11979-2 using a model eye) for the aged LALs both before and after irradiation.[47]

Correction of Higher-order Aberrations With Digital LDD. To determine whether higher-order aberrations could be corrected in the LAL, a digital LDD developed in collaboration with Zeiss-Meditec (Jena, Germany) was tested in vitro (Figure 7). The device is capable of projecting a computer-generated image onto the plane of the LAL at 365 nm. A picture of the digital-light LDD is shown in Figure 7. At the heart of this instrument is the digital mirror device (DMD), which is a pixelated, micromechanical spatial light modulator formed monolithically on a silicon substrate. Typical DMD chips have dimensions of 0.594 × 0.501 inches, and the micromirrors are 13 to 17 mm on an edge and are covered with a reflective aluminum coating. Physically, each mirror can rotate ± 10º. A mirror rotated to +10º reflects incoming light into the projection lens and onto the IOL through the eye. When the mirror is rotated –10º, the reflected light misses the projection lens.

Since the refractive response of the LAL is anticipated to be directly dependent upon the spatial intensity pattern of the light applied, the digital LDD can be used to customize a treatment pattern onto the LAL. One particular area where this ability would be crucial is in the correction of higher-order optical aberrations. To assess the ability of the LAL to correct higher-order aberrations using the digital LDD, the Zernike aberration known as tetrafoil and described by the equation,

$$I_{tetrafoil} = (4\rho^2\text{-}3)\rho^2 \cos 2\theta$$

Where:
ρ is the normalized radial coordinate
θ is the azimuthal angle of the unit circle

was programmed into the DMD, and the LAL was irradiated with this spatial intensity profile.

Another higher-order aberration induced by age-related loss of negative spherical aberration in the cryalline lens is the presence of the spherical aberration. The wavefront of this aberration can be represented by the following Zernike polynomial:

$$I_{tetrafoil} = 6\rho^4\text{-}6\rho^2\text{-}1$$

The effect of this aberration is that light impinging on the periphery of the lens comes to a different focus than light being refracted through the central part of the optic. Applying the principles of geometric optics, one way to minimize spherical aberration is to create an aspheric lens that in its simplest form would possess a radius of curvature difference between the central and peripheral regions. The digital LDD was also tested to see whether it could alter spherical aberration in an LAL.

6. IN VIVO TESTING

A. Biocompatibility Tests

All tests were conducted in accordance with ISO 11979-5 on both nonirradiated and irradiated LAL samples unless otherwise noted.[49]

Ocular Implantation Study in a Rabbit Model. Cataract surgery and postoperative clinical and histopathologic observations were performed in a masked fashion by Dr Nick Mamalis, an ocular pathologist on the faculty of University of Utah Medical School and Director of the Intermountain Ocular Research Center in accordance with generally accepted animal care guidelines and after formal institutional review board approval from the University of Utah. Two groups of 18 New Zealand white rabbits (36 total) each underwent phacoemulsification after general anesthesia. A nonirradiated LAL was placed in the capsular bag of one eye and a control AMO SI-40 silicone IOL (Advanced Medical Optics, Santa Ana, Calif) was implanted in the fellow eye. In one group of 18 rabbits, the LAL was left unirradiated in the eye throughout the duration of the study (group A). In the second group of 18 rabbits (group B), the LAL was irradiated immediately after implantation (first irradiation) and 24 hours later (second irradiation) using a dose and intensity to simulate adjustment and lock-in exposures. Animals were examined at 1 day, 1 week, 2 weeks, 1 month, 3 months, and 6 months by slit lamp and indirect ophthalmoscopy. Any untoward ocular inflammatory changes or other alterations of anterior and posterior segment structures were noted and compared to control eyes.

Examinations of the cornea to evaluate the eyes for possible UV keratitis were performed at 4, 24, and 48 hours, if necessary, following surgery (group B). A drop of fluorescein was instilled in the eye with irradiated LAL and evaluated with a cobalt blue filter on the slit lamp for the presence of superficial punctate keratopathy.

At the end of 3 and 6 months, 9 rabbits from each group were sacrificed. The eyes were then enucleated and placed in a 10% formalin solution. The globes were sectioned and the IOLs were explanted. The globes were processed for histopathologic examination using light microscopy to evaluate the anterior and posterior segments of the eyes. The anterior and posterior segments of each of the rabbit eyes were evaluated for

alterations due to the LAL or secondary to the UV irradiations. The explanted irradiated LALs, nonirradiated LALs, and control IOLs were evaluated by gross microscopy, scanning electron microscopy, and optical performance (see below).

Subcutaneous Implantation Study. The nonirradiated LALs were implanted in subcutaneous tissue of three rabbits for 4 weeks. Four sites were implanted in each rabbit with LALs and negative control samples (polyethylene strips). Subcutaneous tissues were excised, and the implant sites were examined macroscopically. A histopathologic evaluation of representative implant sites from each rabbit was conducted to further define any tissue response.

B. Power Adjustments in Rabbit Model

In order to demonstrate that the nomogram developed in vitro can be reproduced in vivo, several pilot rabbit studies were conducted to correlate the in vitro and in vivo power adjustment. The studies are described below.

*Rabbit Study No. 1***.** This study involved implantation of five LALs in five consecutive rabbit eyes followed by in vivo irradiation of the LALs with a predetermined dose derived from in vitro studies. The rabbits underwent conventional phacoemulsification and were implanted with a 20.0-D LAL in each of the five eyes. After suturing the incision, irradiation of each LAL was performed with an operating microscope–based LDD using the nomogram with a target adjustment of +0.75 D. Immediately after irradiation, the LALs were explanted. Optical characterization and induced dioptric power changes were assessed by Fizeau interferometry 24 hours postirradiation.

*Rabbit Study No. 2***.** This study was designed to (1) evaluate a greater range of power changes, both positive and negative, with the power adjustments and lock-in performed in a clinically acceptable time frame (adjustment performed 2 weeks postimplantation with lock-in the next day) using a prototype surgical microscope-based delivery system, (2) evaluate the stability of the locked-in explanted lenses, and (3) assess the biocompatibility of the material both preadjustment and postadjustment, and the phototoxicity of the irradiation procedure to the cornea and retina. The rabbits underwent conventional phacoemulsification and were implanted with 20.0-D LALs. Two weeks after implantation, power adjustment of the LAL was performed. The following day, lock-in irradiation was performed. Four weeks after lock-in, the rabbits were sacrificed, LALs explanted, and the eyes immersed in formalin for histopathologic study. LAL optical characterization and induced dioptric power changes were assessed by Fizeau interferometry. Explanted LALs were subject to further irradiation sufficient to induce a maximal power change to determine whether further irradiation could induce power changes after lock-in.

RESULTS

1. IN VITRO TESTING

A. Cytotoxicity

Under the conditions of the MEM elution test, the 1X MEM extracts of the irradiated and nonirradiated LALs and saline extracts of the macromer and photoinitiator showed no evidence of causing cell lysis or toxicity. The reagent control, negative control, and the positive control performed as anticipated.

B. Hydrolytic Stability

The results showed that there was no weight loss observed under any of the conditions studied. The percent of extractables by exhaustive extraction of the exposed samples was essentially the same as the unexposed controls. Analysis of the hydrolysate revealed no leached species as detected by HPLC and GC. The light transmission properties remained stable throughout the study.

A representative GC chromatogram of the methylene chloride extract of the nonirradiated test slab is presented in Figure 8, showing multiple peaks of macromer between 15.5 and 28.8 minutes, and a single photoinitiator peak at 33.4 minutes. Methylene chloride is considered to be an excellent solvent for silicone. It is used to determine the total extractables, which include the free macromer, photoinitiator, and any low-molecular-weight unreacted silicone components. On the other hand, aqueous medium such as saline is a nonsolvent for silicone. The macromer, photoinitiator, and silicone are not expected to leach out in an aqueous environment. Figure 9 shows typical GC chromatograms of the methylene chloride extracts of the saline control and hydrolysates from nonirradiated and irradiated samples under different test conditions. There were no peaks observed in the region that matched macromer or photoinitiator, indicating no leached macromer or photoinitiator. In addition, the chromatograms of the hydrolysates were identical to that of the saline subjected to the same temperature conditions as the test samples, further confirming that no other leached species were detected.

C. Photostability

No migrated species were detected in the balanced salt solution (BSS) surrounding the samples during accelerated UV light exposure. A 15-nm shift at 10% T was observed on the exposed samples as compared to the dark controls at the end of the required exposure time. This shift is attributed to the consumption of the photoinitiator as a result of UV light exposure. We do not consider this

shift as significant, since sufficient UV protection for the patient is maintained after 20 years' simulated in vivo exposure. No leached species were associated with the shift.

D. Nd:YAG Laser Exposure Test

The results demonstrated that the response of the LAL Nd:YAG laser exposure was comparable to that of the control commercially available silicone IOL. Chemical analysis of the saline surrounding the LAL during Nd:YAG irradiation showed no leached species by HPLC and GC analysis and was noncytotoxic as determined by MEM elution method.

E. Lens Mechanical Property Assessment

The dimensional and mechanical properties of the LALs were tested in accordance with the FDA Intraocular Lens Guidance Document and ISO 11979-3.[46] The results are summarized below.

Dimensions. All of the dimensional attributes of the LALs were within design specifications and requirements identified in 11979-3.[46]

Mechanical Testing.

- Optic decentration
  0.035 ± 0.030 mm for 11-mm compression
  0.059 ± 0.040 mm for 10-mm compression
- Optic tilt
  0.29 ± 0.27° for 11-mm compression
  0.44 ± 0.34° for 10-mm compression

Loop pull strength: >25 g minimum.

Dynamic Fatigue Durability. All lenses passed the dynamic fatigue testing without incurring any permanent deformation.

Folding/Injection Testing. The LALs were folded with a Nickamin II or Nickamin III foldable lens insertion forceps for 3 minutes before releasing from the folder. The lenses recovered from folding with respect to their dimension and optical properties in 1 hour. The power adjustment performance was not affected by folding.

Surface and Bulk Homogeneity. The LALs were free from surface and bulk defects, and all edges were smooth under 10× magnification using a stereo microscope.

F. Optical Performance Testing

Optical Characterization of Molded LALs. Table I displays the optical performance data of 25 LALs with a target manufacturing power of 20.6 D. These lenses were compression-molded using established manufacturing procedures and then optically characterized in water by LPS, resolution efficiency, and MTF. All measurements were performed in accordance with ISO 11979-2.[47] Inspection of Table I indicates that all of the molded LALs meet or exceed the requirements published by ISO regarding resolution efficiency, dioptric power tolerance, and MTF.

TABLE I: OPTICAL CHARACTERIZATION OF MOLDED LIGHT-ADJUSTABLE LENSES

		AQUEOUS MEASUREMENTS	
LENS NO.	POWER (D)	RES	MTF
1	20.73	G4 E5	0.48
2	20.74	G4 E5	0.50
3	20.72	G4 E5	0.50
4	20.70	G4 E5	0.50
5	20.69	G4 E5	0.47
6	20.63	G4 E5	0.49
7	20.63	G4 E5	0.52
8	20.73	G4 E5	0.51
9	20.63	G4 E5	0.51
10	20.66	G4 E5	0.45
11	20.78	G4 E5	0.49
12	20.64	G4 E5	0.48
13	20.61	G4 E5	0.53
14	20.59	G4 E5	0.48
15	20.62	G4 E5	0.54
16	20.56	G4 E5	0.53
17	20.67	G4 E5	0.50
18	20.55	G4 E5	0.51
19	20.51	G4 E5	0.46
20	20.73	G4 E5	0.53
21	20.63	G4 E5	0.50
22	20.53	G4 E5	0.49
23	20.66	G4 E5	0.53
24	20.64	G4 E5	0.54
25	20.63	G4 E5	0.52
Ave	20.65		0.50
SD	0.07		0.02

MTF, modulation transfer function; RES, resolution.

Nomogram Development: Adjustment and Lock-in. Figure 10 presents a dose response curve developed for a +22 D base power LAL for negative power adjustment. The dose values listed along the x-axis represent the average dose of energy applied to the front surface of the LAL. At each of the doses indicated, 30 LALs were irradiated. One of the striking features of this plot is the ability of the LAL to be adjusted in approximate 0.25-D increments in the range –0.5 to –2.0 D with a maximal standard deviation of 0.12 D.

Table II shows examples of positive adjustments. For the current formulation, a more extensive nomogram has been developed for negative adjustments; however, preliminary data demonstrate that reproducible positive adjustments have been made at two sample doses as indicated.

Table III demonstrates the results of 20 LALs adjusted with the same dose and then photolocked. At this dose, the mean change in power was –1.14 D (SD, 0.10 D). Analysis of the data indicates that the LALs can be

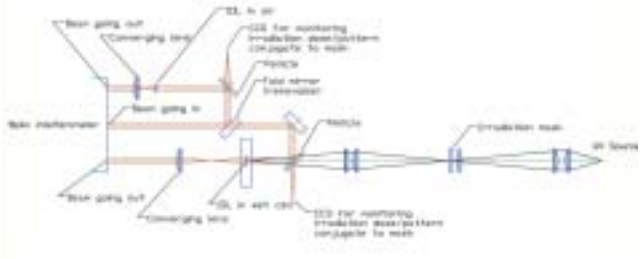

FIGURE 5

Schematic of interferometer/irradiation system for power adjustment and lock-in nomogram development. The instrument is built around a commercial Fizeau interferometer (WYKO 400) fitted with a transmission flat. The instrument possesses both an irradiation projection system and an optical analysis package. The light source employed in the irradiation of the light-adjustable lens (LAL) is a mercury arc lamp fitted with a liquid-filled fiber optic light guide and a 365-nm interference filter (±10-nm bandpass for characterizing the LAL). A tracer beam with wavelengths not absorbed by the photoinitiator is placed colinear with the irradiation path, and a CCD camera mounted to a beam splitter microscope assembly is included to aid in intraocular lens (IOL) alignment. The camera also allows viewing and recording of the entire lens before, during, and after irradiation. Plane, collimated light exiting from the interferometer is brought to a focus using a 2.5× (f/No. = 7.1) microscope objective. This microscope objective is mounted on an x, y translation stage so that once the power of the IOL is changed, the focus of the objective can be moved to allow the IOL under test to collimate the light into a plane wave. The collimated light leaving the IOL is returned back along the centerline of the interferometer by a pellicle beam splitter and a fold mirror and finally recombined with the reference beam inside the interferometer. Each analysis part of the arm contains a lens wheel that allows eight different lenses to be placed into each optical arm of the interferometer. After an IOL is irradiated, an interferogram will be used to measure power changes and potential aberrations in the lens induced by the irradiation.

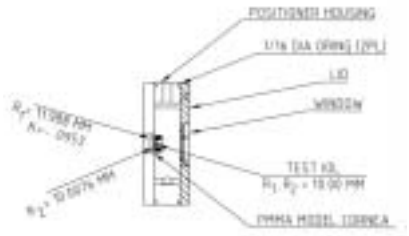

FIGURE 6

Model eye for nomogram development.

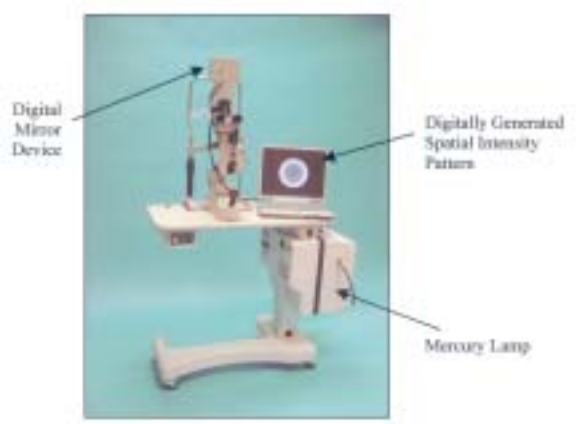

FIGURE 7

Digital light delivery device. This device is similar to the analog device (Figure 3), except that the irradiation pattern is programmed digitally rather than using a variable neutral density filter.

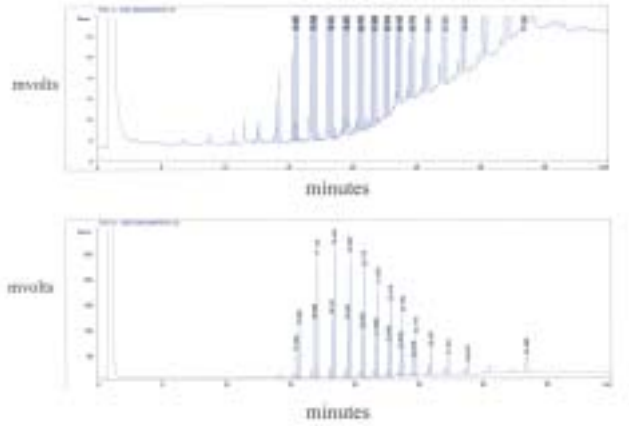

FIGURE 8

Gas chromatograms of methylene chloride extract of light-adjustable lens (LAL) test slab showing multiple macromer peaks between 15.5 and 28.8 minutes, and a single photoinitiator peak at 33.4 minutes. Top chromatogram shows a full vertical scale of 20 mV, and bottom shows a full scale of 300 mV. The x-axis denotes retention time in minutes.

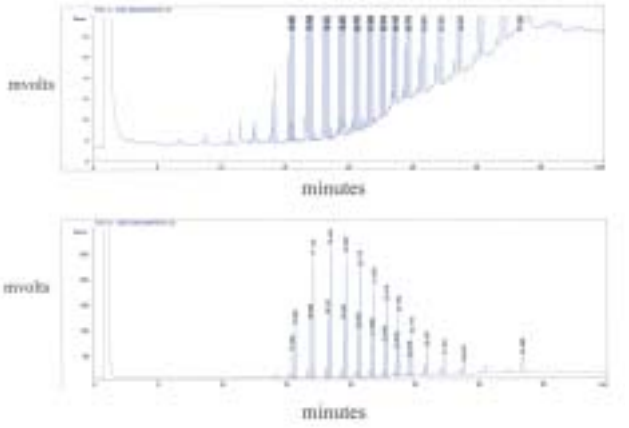

FIGURE 9

Gas chromatograms of (top) saline, (center) nonirradiated hydrolysate, and (bottom) irradiated hydrolysate samples.

adjusted and photolocked with reproducibility; the resolution efficiencies and MTF values of the lenses meet the acceptable limits set forth by the ISO guidelines. A graphical example of the ability of the LAL to maintain high contrast is depicted in Figure 11, which plots the MTF of a representative LAL through the treatment and photolocking procedure. For comparison, a standard +20 D AMO SI40 (Advanced Medical Optics, Santa Ana, Calif) IOL is also plotted.

TABLE II: SAMPLE POSITIVE POWER ADJUSTMENTS FOR A +22 DIOPTER LIGHT-ADJUSTABLE LENS

DOSE 300 mJ/cm²		DOSE 900 mJ/cm²	
LENS NO.	POWER CHANGE (D)	LENS NO.	POWER CHANGE (D)
1	0.72	1	1.83
2	1.11	2	1.80
3	1.06	3	2.03
4	1.09	4	1.81
5	0.98	5	2.03
6	0.91		
7	1.17		
8	0.94		
9	1.01		
10	1.3		
11	0.94		
12	0.88		
13	1.02		
14	1.17		
Ave	1.02	Ave	1.90
SD	0.15	SD	0.12

G. Effectiveness of Lock-in Procedure and Solar Protection

The power of the locked LALs that were exposed in the solar simulator at an intensity of 0.3 mW/cm² at 37°C in water for a period of 900 consecutive hours or 300 calculated in vivo days remained stable. The resolution and MTF of the solar exposed LALs were comparable to those before exposure.

Following lock-in, the total extractable analysis of the locked LALs by exhaustive extraction using methylene chloride solvent revealed that the residual macromer and photoinitiator levels were less than 1%, further confirming the lack of reactivity and stability of the locked LALs.

The results show that the LAL has a minimum of 2 hours protection under which the lens would not change power if the patients forget to wear sunglasses during midday sun exposure.

H. Stability and Predictability of LAL on the Shelf

Lens dimensions (overall diameter and haptic angle), optical performance BFL, resolution, and MTF, and power adjustment performance of the stored LALs remained stable and were comparable to those freshly manufactured. Table IV presents the power adjustment data of the aged LAL as compared to the freshly manufactured LAL. The data confirm that the LALs main-

TABLE III: ADJUSTMENT AND LOCK-IN OF 22.5-D LIGHT-ADJUSTABLE LENS*

120-SECOND ADJUSTMENT				POST LOCK-IN		
LENS NO.	D POWER	WET RESOLUTION	MTF @ 100 lp/mm	D POWER DRIFT	WET RESOLUTION	MTF @ 100 lp/mm
1	-1.1	G4-E4	0.48	-0.14	G4-E4	0.47
2	-1.13	G4-E4	0.53	-0.06	G4-E4	0.55
3	-1.1	G4-E4	0.49	-0.26	G4-E4	0.47
4	-1.06	G4-E4	0.53	-0.33	G4-E4	0.51
5	-1.07	G4-E4	0.52	-0.25	G4-E4	0.45
6	-1.22	G4-E4	0.51	-0.19	G4-E4	0.5
7	-1.3	G4-E4	0.5	-0.3	G4-E4	0.48
8	-1.35	G4-E4	0.44	-0.26	G4-E4	0.52
9	-1.27	G4-E4	0.49	-0.25	G4-E4	0.49
10	-1.14	G4-E4	0.46	-0.12	G4-E4	0.48
11	-1.09	G4-E4	0.51	-0.12	G4-E4	0.52
12	-0.96	G4-E4	0.52	-0.27	G4-E4	0.49
13	-1.06	G4-E4	0.47	-0.22	G4-E4	0.52
14	-1.05	G4-E4	0.56	-0.33	G4-E4	0.53
15	-1.08	G4-E4	0.46	-0.22	G4-E4	0.49
16	-1.27	G4-E4	0.53	-0.35	G4-E4	0.49
17	-1.15	G4-E4	0.46	-0.29	G4-E4	0.47
18	-1.12	G4-E4	0.51	-0.33	G4-E4	0.51
19	-1.12	G4-E4	0.51	-0.18	G4-E4	0.53
20	-1.2	G4-E4	0.5	-0.11	G4-E4	0.45
Ave	-1.14		0.50	-0.23		0.50
SD	0.10		0.03	0.08		0.03

MTF, modulation transfer function.
*Resolution efficiency and MTF are maintained through adjustment and lock-in.

TABLE IV: LIGHT-ADJUSTABLE LENS SHELF-LIFE STABILITY: POWER-ADJUSTMENT PERFORMANCE TESTING

	PREIRRADIATION				POSTIRRADIATION	
LENS ID	RESOLUTION EFFICIENCY	MTF (mJ/cm^2)	IRRADIATION DOSE CHANGE	FINAL DIOPTRIC EFFICIENCY	RESOLUTION	MTF
Fresh LALs	G4 E5	0.50 ± 0.02	1,200	–1.03 ± 0.18	G4 E4	0.50 ± 0.04
Aged LALs (4.5 mo)	G4 E5	0.50 ± 0.01	1,200	–0.99 ± 0.18	G4 E4	0.53 ± 0.02

MTF, modulation transfer function.

tained resolution efficiency and MTF above those established in the ISO guidelines, and are stable as a function of storage.

I. Correction of Higher-order Aberrations With Digital LDD

Figure 12A shows a grayscale digital image of an astigmatic pattern that is projected onto the LAL. This pattern was input to the DMD chip of the breadboard system and projected onto the LAL. In Figure 12B, a 3-dimensional color image of the preirradiation wavefront of the LAL is depicted. The wavefront was remeasured 24 hours postirradiation, and Figure 12C shows the astigmatic or saddle-shaped wavefront of the irradiated LAL. The LAL was positioned at a place of best focus for the entire wavefront, which is intermediate between the tangential and sagittal wavefronts, respectively. One meridian has a wavefront converging, and the other meridian has the wavefront diverging.

Figure 13A shows the grayscale digital representation of the tetrafoil Zernike term that was applied to the LAL. Figures 13B and 13C show the interference fringes before and after irradiation with the tetrafoil spatial intensity pattern, respectively. Comparison between this set of interference fringes shows that projected spatial intensity profile was reproduced on the wavefront of the LAL. To further illustrate this point, the 3-dimensional wavefront calculated from the interference fringes shown in Figure 13C is displayed in Figure 13D. This shows the fourfold symmetry of the wavefront.

Figure 14 demonstrates reduction of spherical aberration. Figure 14A shows the interference fringes from a +20.5 D LAL, preirradiation. Inspection of this interference pattern shows that there is only 1 fringe in the central 4 mm of the optic and approximately 4 fringes (2 waves) due to spherical aberration at the periphery of the LAL. Figure 14B shows an LAL that was irradiated over its periphery to change the radius of curvature on the outside portion of the LAL, so as to reduce the amount of spherical aberration. Inspection of this figure shows the removal of 2 fringes (1 wave) of spherical aberration due to the irradiation.

2. IN VIVO TESTING

A. Ocular Implantation Study Using a Rabbit Model

All of the rabbits in this study (groups A and B) underwent uncomplicated implantation of an LAL in one eye and a control three-piece silicone lens in the opposite eye. Group B eyes were implanted with an LAL and then underwent immediate adjustment light exposure as well as additional irradiation to simulate lock-in 1 day following surgery. Each of the rabbits in the study group, as well as the control group, tolerated the surgery well with no untoward effects.

Slit-lamp examination results on these animals at 1 and 2 weeks and 1, 3, and 6 months reveal no clinically significant difference between LALs and control silicone IOLs. As is commonly seen in the rabbit model of IOL implantation, by the 3-month examination both groups of animals began to show significant posterior synechia formation as well as associated iris bombé. Both groups also showed a small increase in iris vasculature and inflammatory deposits on the IOL surface. These trends continued at the 6-month examination without any differences between the study and control groups.

Histopathologic evaluation of the rabbit eyes in both groups showed no sign of any toxicity or inflammatory reaction in either the anterior or the posterior segments of the rabbit globes. Group B eyes that underwent irradiation of the study LAL showed no difference compared to the control IOL group. Rabbits in both groups showed significant posterior synechia formation with iris bombé formation in several cases. There was also a mild amount of proliferative cortical material in the fornix of the lens capsular bag forming a mild Soemmering's ring, which is a common finding 6 months postoperatively in the rabbit cataract surgery model.

Scanning electron microscopic analysis of the explanted study LALs showed a well-finished optic and loop optic junction with no obvious abnormalities on the

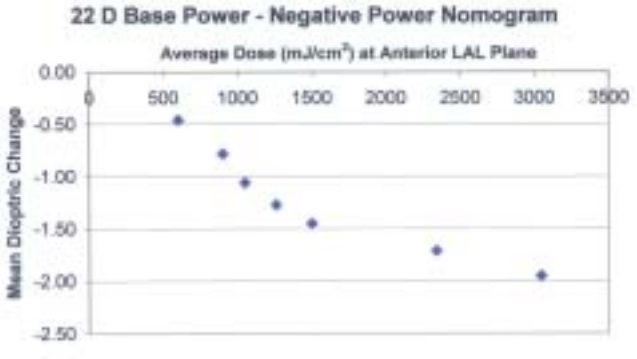

FIGURE 10

Sample negative power adjustment nomogram for a +22 diopter light-adjustable lens.

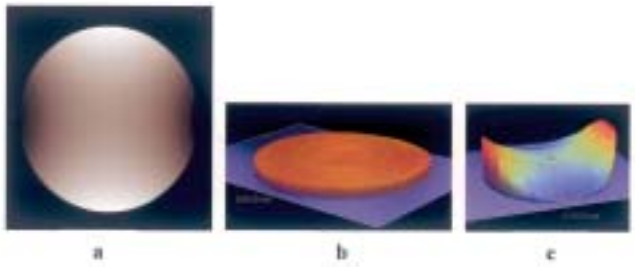

FIGURE 12

Creation of toric light-adjustable lens (LAL: A, Digital image projected on to the LAL. This pattern was input to the Digital mirror device chip of the breadboard system and projected out onto the LAL. B, Three-dimensional image of preirradiation wavefront. C, Three-dimensional image of postirradiation wavefront, representing 1.37 D of induced cylinder.

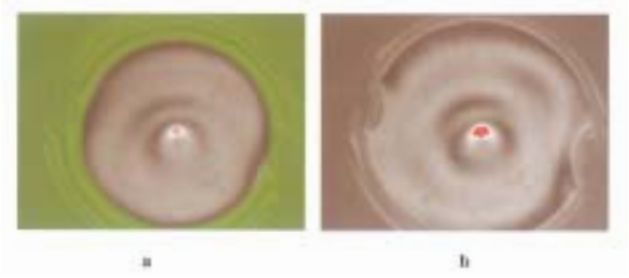

FIGURE 14

Reduction of spherical aberration in light-adjustable lens (LAL) using digital light delivery device. A, Four waves of spherical aberration at the LAL periphery. B, Removal of 2 fringes (1 wave) of spherical aberration following irradiation of the LAL periphery.

surface of the implant. The lens compared favorably to the control silicone IOLs when evaluated by scanning electron microscopy. The scanning electron micrographs of the explants are shown in Figure 15.

In summary, implantation of the LAL alone (group A), or followed by UV irradiation and lock-in (group B), was successfully performed in all of the eyes in this rabbit model. The fellow eyes similarly underwent successful implantation and follow-up of a control three-piece silicone IOL. There was no sign of any untoward inflamma-

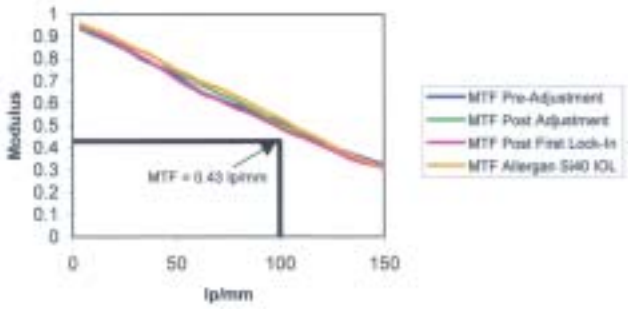

FIGURE 11

In vitro modulation transfer function (MTF) comparison between the light-adjustable lens through adjustment and photolocking, and a commercial AMO SI40 intraocular lens (Advanced Medical Optics, Santa Ana, Calif).

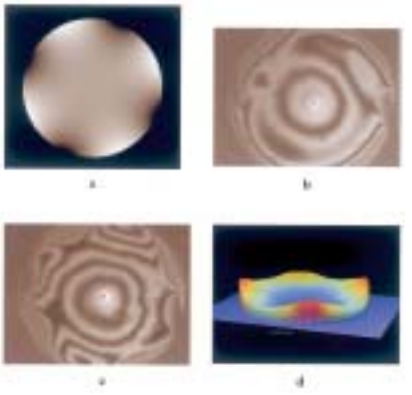

FIGURE 13

A, Digital grayscale of tetrafoil intensity pattern projected onto light-adjustable lens. Interferogram before (B) and after (C) irradiation. D, Three-dimensional spatial representation of tetrafoil wavefront.

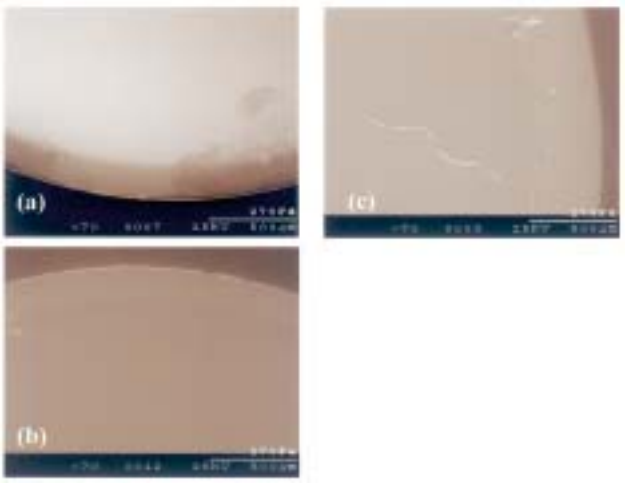

FIGURE 15

Scannning electron micrographs of 6-month explants at 70×. Nonirradiated and irradiated light-adjustable lenses (A and B) showed a well-finished optic with no obvious abnormalities on the surface of the implant. Lens compared favorably to control silicone intraocular lenses (C).

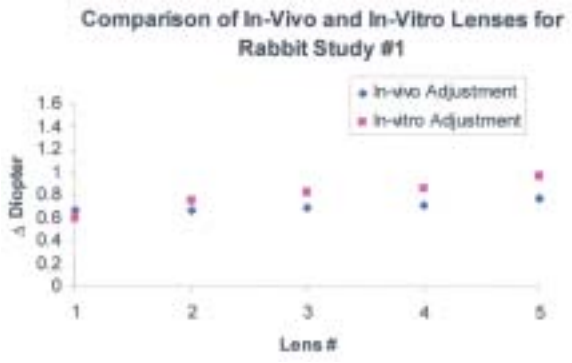

FIGURE 16
Comparison of in vivo and in vitro power change in 20.5-D light-adjustable lens.

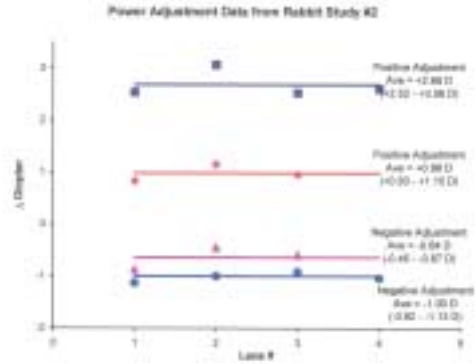

FIGURE 17
Power adjustments achieved from rabbit study No. 2.

tory cell reaction in either the study or the control lens groups. There was no sign of any toxicity from the light exposure in either the anterior segment or the posterior segment of group B eyes. Histopathologic evaluation of both LAL groups revealed no signs of tissue damage or untoward inflammatory reactions.

B. Power Adjustments in Rabbit Model

Rabbit Study No. 1. The resultant in vivo lens power change of 0.71 ± 0.05 D was found to be in close agreement with the in-vitro power change of 0.80 ± 0.14 D (Figure 16). These data suggest that LAL lens power adjustments can be reproducibly achieved in vivo and that in vitro data is predictive of the in vivo response.

Rabbit Study No. 2. Figure 17 shows results of myopic and hyperopic power adjustments in small series of rabbits for each dose of irradiation. A range of positive and negative power adjustments can be reproducibly attained within approximately ±0.25 D in implanted lenses. The efficacy of the lock-in procedure was demonstrated by the absence of any significant lens power changes of adjusted, locked-in lenses subjected to a reirradiation dose sufficient to produce +2.68 D change in a fresh nonirradiated lens. Slit-lamp examinations and histopathologic results demonstrated that both the nonirradiated and irradiated LALs were well tolerated in the rabbit eyes for 4 weeks postadjustment/lock-in exposure, as compared to commercially available control silicone lenses. These data confirm the biocompatibility of the LAL material and the nontoxicity of the power adjustment/lock-in irradiation treatments.

C. Subcutaneous Implantation Study

Clinical Observations. All animals appeared clinically normal throughout the duration of the study. Body weight data for individual rabbits were considered acceptable.

Macroscopic Observations. There was no visible reaction at any test or control site. This resulted in a macroscopic reaction of "not significant" tissue contact irritation.

Microscopic Observations. The LAL was a nonirritant as microscopically compared to the control implant material.

DISCUSSION

The results establish that a biocompatible silicone IOL can be fabricated that is precisely adjustable using safe levels of light. Specifically, a silicone matrix embedded with photosensitive silicone macromers and conjugated UV blockers is capable of precise positive and negative power adjustment in vitro to within approximately 0.25 D. After adjustment, lock-in irradiation is performed with mean power drift of <0.25 D and stabilization of IOL power against alteration from solar exposure. Implantation of LALs in rabbits reveals excellent biocompatibility after 6 months that is comparable to a commercially available silicone IOL.

Since the LAL was designed to mimic conventional silicone IOLs, except in its capacity for adjustment, the LAL's mechanical properties required assessment. The blend of macromers and silicone matrix might have been expected to alter these properties and make the LAL unsuitable for clinical use. Testing of mechanical properties, including compression force, axial displacement in compression, optic decentration, optic tilt, angle of contact, compression force decay, dynamic fatigue durability, loop pull strength, surface and bulk homogeneity, and folding and injection testing, revealed no significant differences from commercial controls.

Because of the concern about leaching of macromers, photoinitiator, and/or UV blockers from the LAL, hydrolytic stability testing was performed. Results at 3 months in BSS solution at 50°C showed no evidence of leaching by HPLC and GC analysis. Photostability testing of the LAL was also conducted. LAL samples exposed in a solar simulator at 37°C to simulate a 20-year in vivo

exposure showed no leaching in BSS. Testing to assess for leaching during Nd:YAG irradiation likewise showed no leaching into BSS by HPLC and GC analysis, and the solution was noncytotoxic.

Given that patients implanted with the LAL would wait, on the average, 2 to 4 weeks before adjustment and lock-in, they risk inadvertent exposure to sunlight during this time before lock-in is completed. Sunglasses that block out UV-A light in the wavelength range that activates the photoinitiator would be worn during this time. Since some patients may walk outside and forget to wear sunglasses prior to lock-in, we tested how long the LAL could be exposed to bright solar irradiation without changing shape. The LAL could endure at least 2 hours exposure to UV light, equivalent to that found at peak midday solar exposure, without optical change.

The analog light delivery systems in both operating microscope and slit-lamp designs are effective and safe. Adjustments using the operating microscope system in rabbits produce reproducible positive and negative power changes in small series of animals. Furthermore, tests of irradiation safety in rabbits for both adjustment and lock-in reveal no clinical or histopathologic evidence of ocular toxicity.

In collaboration with Zeiss-Meditec, Inc, a digital light delivery system was tested to correct astigmatism and higher-order aberrations. In vitro testing demonstrated correction of cylinder, tetrafoil, and spherical aberrations in the LAL.

LAL technology has broad potential application across the field of IOLs. For patients undergoing cataract extraction, an adjustable monofocal IOL would afford them assurance against wearing spectacles for either distance or near (but not both) after surgery. Except for the need to wear protective sunglasses until lock-in is completed, clinical use of LAL technology would be the same as for a conventional IOL. At 2 to 4 weeks when spectacles are ordinarily prescribed, patients would undergo a power adjustment that would last approximately 30 to 120 seconds, depending on the specific refractive error. During the next 12 to 15 hours after adjustment, macromers would migrate into the treated region to obtain the desired refractive result. One day after adjustment, when the macromers have diffused to equalize their concentration throughout the LAL matrix, the correct adjustment is confirmed and the LAL's final power is locked in with a 60- to 120-second dose across the entire lens. One day following lock-in, the patient could have unlimited exposure to ambient UV light without fear of further changes in LAL power.

While not addressed in these studies, additional adjustments can be made on the LAL until lock-in. With initial adjustment, approximately 10% to 20% of the macromer is polymerized (data not shown). Since there is substantial macromer that persists after adjustment, additional treatments can be performed that polymerize residual macromer and effect further changes in lens shape. For example, if a postoperative myopic refractive error is overtreated with irradiation of the LAL periphery to flatten the central optic and induce hyperopia, a second irradiation directed at the central portion of the LAL would increase its power and return the patient to emmetropia. Preliminary studies (not included above) have indicated that approximately 80% of maximal adjustment can be obtained with a second treatment.

Retreatment of the LAL might not only be useful to fine-tune an adjustment, but also allow patients to try a particular refractive correction before accepting or rejecting it. For example, patients might wish to try monovision. A LAL powered for near could be implanted and adjusted to optimize near correction; if after attempting monovision, the patient preferred emmetropic correction in the operated eye, the LAL could be retreated to reduce its power to plano.

Reversibility of the refractive change might also be useful for trying multifocality. Multifocal IOLs (eg, AMO Array, Santa Ana, Calif) have met with some success in patients desiring near and distance vision without using spectacles.[12,17-19] Broad acceptance of this technology has been hampered, in part, by inability to predictably achieve emmetropia and inability to reverse the multifocal effect for those patients who cannot tolerate it. Patients intolerant to multifocality sometimes require IOL exchange with a monofocal lens.[13] As established above, the LAL enables creation of a multifocal optic in situ after adjusting the LAL to emmetropia. Were the patient not to tolerate multifocality, the edges of the LAL could be treated to remove the multifocal optic and recreate a monofocal LAL. Customization of the treatment pattern using the digital LDD would probably facilitate both creating and removing a multifocal optic. Furthermore, customization would allow optimization for pupillary diameter and any decentration of the optic.[50,51]

Retreatment of the LAL would also be desirable in the long-term management of pediatric cataract. While IOL implantation in pediatric cataract has been increasingly utilized in infants, myopic shifts greater than 5 D occur secondary to ocular growth.[52-54] In vitro studies of the LAL demonstrate up to 4 D of myopic power adjustment with one adjustment (data not shown). With subsequent adjustments, potentially larger dioptric shifts could be obtained. With the current LAL formulation, however, readjustment(s) during the first 6 years of life would not be practical because of the unpredictable effects of ambient light exposure to LAL power. To permit periodic adjustments over many years, the LAL formulation would

have to be changed such that ambient light would not be sufficient to induce a power change. Such formulation changes are possible to obtain and constitute an important goal for a second-generation LAL.

Based on pilot trials of the LAL in a rabbit model for correction of myopia, in vitro nomograms were predictive of the in vivo dose response. This apparent tight correlation of in vitro and in vivo data is probably related to reproducibility of the photosensitive macromer's response to irradiation, whether in or outside of the eye. Light-adjustable silicones, such as the LAL, involve interaction of light with inert materials. This is different from and inherently more predictable than the interaction of light with biological material, as occurs in excimer laser or thermal laser used in retinal applications. Certainly, there may be some variance of corneal light transmission in aged patients; however, we have shown that corneal transmission variance of ±10% has no effect on power adjustment. The probable correlation between in vitro and in vivo nomograms suggests that detailed in vitro nomograms can be developed and will be predictive of their in vivo counterparts. This may reduce the need to develop nomograms empirically on patients implanted with the LAL.

While diagrammatically the LDD is shown to treat either the center or the periphery of the LAL for correction of hyperopia and myopia, respectively (Figures 1 and 2), in actuality light is spatially distributed across the entire optic during adjustment. This is achieved with variable neutral density (apodizing) filters that rotate into place after the patient's refractive error is entered onto the display panel. Separate filters are used for correction of hyperopia and myopia and lock-in. With a specific filter in place, power change varies as a function of intensity and duration of treatment. Correction of combined spherical and toric errors would require almost an infinite collection of such apodizing filters; thus, customization of the UV light pattern using the digital LDD is particularly important to address spherocylindrical refractive error. The digital LDD enables a customized computer-generated spatial intensity pattern to be "written" accurately onto the LAL. As we optimize spatial patterns to treat combined spherical and toric errors, these can be readily generated with the digital LDD to treat individual refractive errors. Digital LDD customized LAL adjustment could also be applied to compensate for irregular astigmatism, such as after corneal transplantation, radial keratotomy, or irregular corneal ablations. Similarly, wavefront-based adjustments could be made in the LAL using a digital LDD. Unlike excimer laser correction of higher-order aberrations in the cornea, refractive correction in the LAL would not be subject to the unpredictability of wound healing.[55,56]

There are limitations to LAL technology. While adjustment can be tailored to any size optical zone, lock-in requires treatment of the entire optic. Thus, patients must dilate at least 6 mm postoperatively to effect lock-in with the LDD. Patients with poor dilation preoperatively, such as those taking miotics, with posterior synechiae, or with pseudoexfoliation, would not be good candidates for LAL implantation. There will be additional patients who dilate well preoperatively but have small pupils postoperatively. Some of these would be predictable based on complicated surgery with hemorrhage or iris trauma; others, however, would be surprises. While this population of postdilation "surprises" might be small, provisions for adjustment and lock-in would have to be developed. Adjustment is feasible with a small pupil, but lock-in requires access to the entire optic. We have considered developing a gonioscopic-like device that would reflect light out to the LAL periphery. This would work probably for those pupils that dilated between 4 and 5.5 mm, but not as well for smaller pupils. Either special optical designs would be required for these smaller pupils, or else patients could be locked in after dilation with iris hooks.

A similar issue would arise in patients developing anterior capsular fibrosis. Silicone IOLs develop more anterior capsular shrinkage and fibrosis than acrylic IOLs.[57-59] Significant anterior capsular opacification can develop as early as 1 month, blocking access of UV irradiation to the entire LAL. Anterior capsular polishing and use of a larger capsulorrhexis can minimize this potential problem.[60,61] Also, adjustment and lock-in can be performed at 2 weeks, before opacification develops.

Currently, new phakic IOL designs are emerging for treatment of high myopia and hyperopia. Novel accommodative IOLs are also in clinical trials for treatment of presbyopia.[62,63] While success of these designs remains uncertain, should one or more of these IOLs be widely used by ophthalmologists, their adoption will be enhanced if they are made of light-adjustable materials.

We now successfully have implanted our first two patients with LALs and eagerly anticipate a full-scale clinical trial in the next few months.

SUMMARY

An LAL and LDD (analog and digital) have been developed to adjust the power of a silicone IOL noninvasively during the postoperative period.

LAL power can be adjusted and locked in over a range of 4 D (–2 to +2 D) with one light adjustment. Following adjustment, optical quality is maintained.

The LAL is biocompatible in a rabbit model. There is no evidence of macromer, UV blocker, or photoinitiator leaching in hydrolytic stability testing.

The LAL is comparable to a commercially available silicone IOL in terms of its mechanical properties.

Preliminary testing of the LAL in vivo demonstrates reproducible spherical power adjustment across a range of myopic and hyperopic refractive errors.

Use of a digital LDD enables correction of higher-order aberrations, including toric errors, tetrafoil, and spherical aberrations.

Use of LAL technology may enhance visual outcome for patients treated with IOLs for correction of aphakia, refractive errors, and presbyopia.

ACKNOWLEDGEMENT

This research grew out of a collaboration I established with Robert Grubbs, PhD, and Julia Kornfield, PhD, at the California Institute of Technology (Cal Tech) in 1996. After developing the idea of a light-adjustable IOL and searching for material scientist collaborators at the University of California, Berkeley, and Stanford University, I was fortunate to engage the outstanding scientists at Cal Tech to help solve the problem of noninvasive IOL adjustability. Drs Grubbs and Kornfield formulated an ingenious approach to the problem, and I joined them in supervising two postdoctoral students (Jagdish Jethmalani, PhD, and Christian Sandstedt, PhD) for 3 years as the technology was developed. I participated from the University of California, San Francisco, and would fly down once or twice a month to meet with the team. Once we had made some progress and filed a series of patents, we started Calhoun Vision, Inc, Pasadena, Calif, to further develop and commercialize the LAL. Starting in 1999, I joined the team in Pasadena nearly weekly to review laboratory studies and help guide our research efforts. All the work presented herein has been performed in the past 2 years at Calhoun Vision.

I gratefully acknowledge Shiao Chang, PhD, and Christian Sandstedt, PhD, and the employees of Calhoun Vision, Inc, who conducted the in vitro experiments described in this thesis. Drs Sandstedt and Chang also provided significant input into the "Methods" and "Results" sections. Finally, I thank Dr Nick Mamalis of the University of Utah for conducting LAL implantations, irradiations, postoperative evaluation, and histopathologic analysis of the enucleated globes.

REFERENCES

1. Spalton D, Koch D. The constant evolution of cataract surgery. *BMJ* 2000;321(7272):1304.
2. Brandser R, Haaskjold E, Drolsum L. Accuracy of IOL calculation in cataract surgery. *Acta Ophthalmol Scand* 1997;75(2):162-165.
3. Olsen T, Bargum R. Outcome monitoring in cataract surgery. *Acta Ophthalmol Scand* 1995;73(5):433-437.
4. Wegener M, Alsbirk PH, Hojgaard-Olsen K. Outcome of 1000 consecutive clinic- and hospital-based cataract surgeries in a Danish county. *J Cataract Refract Surg* 1998;24(8):1152-1160.
5. Murphy C, Tuft SJ, Minassian DC. Refractive error and visual outcome after cataract extraction. *J Cataract Refract Surg* 2002;28(1):62-66.
6. Olsen T. Sources of error in intraocular-lens power calculation. *J Cataract Refract Surg* 1992;18(2):125-129.
7. Pierro L, Modorati G, Brancato R. Clinical variability in keratometry, ultrasound biometry measurements, and emmetropic intraocular-lens power calculation. *J Cataract Refract Surg* 1991;17(1):91-94.
8. Mendivil A. Intraocular lens implantation through 3.2 versus 4.0 mm incisions. *J Cataract Refract Surg* 1996;22(10):1461-1464.
9. Elder MJ. Predicting the refractive outcome after cataract surgery: the comparison of different IOLs and SRK-II v SRK-T. *Br J Ophthalmol* 2002;86(6):620-622.
10. Connors R III, Boseman P III, Olson RJ. Accuracy and reproducibility of biometry using partial coherence interferometry. *J Cataract Refract Surg* 2002;28(2):235-238.
11. Lundstrom M, Barry P, Leite E, et al. 1998 European cataract outcome study: report from the European Cataract Outcome Study Group. *J Cataract Refract Surg* 2001;27(8):1176-1184.
12. Steinert RF, Aker BL, Trentacost DJ, et al. A prospective comparative study of the AMO ARRAY zonal-progressive multifocal silicone intraocular lens and a monofocal intraocular lens. *Ophthalmology* 1999;106(7):1243-1255.
13. Mamalis N. Complications of foldable intraocular lenses requiring explantation or secondary intervention—2001 survey update. *J Cataract Refract Surg* 2002;28(12):2193-2201.
14. Hoffer KJ. Biometry of 7,500 cataractous eyes. *Am J Ophthalmol* 1980;90(3):360-368.
15. Sun XY, Vicary D, Montgomery P, et al. Toric intraocular lenses for correcting astigmatism in 130 eyes. *Ophthalmology* 2000;107(9):1776-1781.
16. Till JS, Yoder J Jr, Wilcox TK, et al. Toric intraocular lens implantation: 100 consecutive cases. *J Cataract Refract Surg* 2002;28(2):295-301.
17. Javitt JC, Steinert RF. Cataract extraction with multifocal intraocular lens implantation: a multinational clinical trial evaluating clinical, functional, and quality-of-life outcomes. *Ophthalmology* 2000;107(11):2040-2048.
18. Javitt JC, Wang F, Trentacost DJ, et al. Outcomes of cataract extraction with multifocal intraocular lens implantation—functional status and quality of life. *Ophthalmology* 1997;104(4);589-599.
19. Jacobi PC, Dietlein TS, Luke C, et al. Multifocal intraocular lens implantation in prepresbyopic patients with unilateral cataract. *Ophthalmology* 2002;109(4):680-686.
20. Hoffman RS, Fine IH, Packer M. Refractive lens exchange with a multifocal intraocular lens. *Curr Opin Ophthalmol* 2003;14(1):24-30.
21. Packer M, Fine IH, Hoffman RS. Refractive lens exchange with the array multifocal intraocular lens *J Cataract Refract Surg* 2002;28(3):421-424.

22. Dick HB, Gross S, Tehrani M, et al. Refractive lens exchange with an array multifocal intraocular lens. *J Refract Surg* 2002;18(5):509-518.
23. O'Brien TP, Awwad ST. Phakic intraocular lenses and refractory lensectomy for myopia. *Curr Opin Ophthalmol* 2002;13(4):264-270.
24. Uusitalo RJ, Aine E, Sen NH, et al. Implantable contact lens for high myopia. *J Cataract Refract Surg* 2002;28(1):29-36.
25. Davidorf JM, Zaldivar R, Oscherow S. Posterior chamber phakic intraocular lens for hyperopia of +4 to +11 diopters. *J Refract Surg* 1998;14(3):306-311.
26. Landesz M, Worst JG, van Rij G. Long-term results of correction of high myopia with an iris claw phakic intraocular lens. *J Refract Surg* 2000;16(3):310-316.
27. Seitz B, Langenbucher A. Intraocular lens power calculation in eyes after corneal refractive surgery. *J Refract Surg* 2000;16(3):349-361
28. Seitz B, Langenbucher A. Intraocular lens calculations status after corneal refractive surgery. *Curr Opin Ophthalmol* 2000;11(1):35-46.
29. Gimbel HV, Sun R, Furlong MT, et al. Accuracy and predictability of intraocular lens power after photorefractive keratectomy. *J Cataract Refract Surg* 2000;26(8):1147-1151.
30. Odenthal MT, Eggink CA, Melles G, et al. Clinical and theoretical results of intraocular lens power calculation for cataract surgery after photorefractive keratectomy for myopia. *Arch Ophthalmol* 2002;120(4):431-438.
31. Kraser GN, inventor; Cooper Vision Inc, assignee. Small incision intraocular lens with adjustable refractive power. US patent 4,950,289. 1990.
32. Eggleston HC, Day T, inventors; Harry C. Eggleston, assignee. Adjustable and removable intraocular lens implant. US patent 5,628,798. 1997.
33. Eggleston HC, Day T, inventors; Harry C. Eggleston, assignee. Adjustable intraocular lens implant with magnetic adjustment facilities. US patent 5,800,533. 1998.
34. O'Donnell FE, inventor. In vivo modification of refractive power of an intraocular lens implant. US patent 5,549,668. 1996.
35. O'Donnell FE, inventor. In vivo modification of refractive power of an intraocular lens implant. US patent 5,725,575. 1998.
36. Johnson DR, inventor. Laser adjustable intraocular lens and method of altering lens power. US patent 4,575,373. 1986.
37. Peyman GA, inventor. Variable refractive power, expandable intraocular lenses. US patent 4,685,921. 1987.
38. Jethmalani J, Grubbs RH, Sandstedt CA, Kornfield JA, Schwartz DM, inventors; California Institute of Technology and the Regents of the University of California, assignee. Lenses capable of post-fabrication power modification. US patent 6,450,642. 2002.
39. Schwartz DM, Jethmalani JM, Sandstedt CA, et al. Post implantation adjustable intraocular lenses. *Ophthalmol Clin North Am* 2001;14(2):339-345.
40. Nishi O, Nishi K, Sakanishi K. Inhibition of migrating lens epithelial cells at the capsular bend created by the rectangular optic edge of a posterior chamber intraocular lens. *Ophthalmic Surg Lasers* 1998;29(7):587-594.
41. Vargas LG, Peng Q, Apple DJ, et al. Evaluation of 3 modern single-piece foldable intraocular lenses: clinicopathological study of posterior capsule opacification in a rabbit model. *J Cataract Refract Surg* 2002;28(7):1241-1250.
42. Izak AM, Werner L, Apple DJ, et al. Loop memory of haptic materials in posterior chamber intraocular lenses. *J Cataract Refract Surg* 2002;28(7):1229-1235.
43. Zuclich JA, Connolly JS. Ocular damage induced by near ultravioltet laser radiation. *Invest Opthalmol* 1976;15:9,760-764.
44. Ham WT Jr, Mueller HA, Ruffolo JJ Jr, et al. Action spectrum for retinal injury from near-ultraviolet radiation in the aphakic monkey. *Am J Ophthalmol* 1982;93(3):299-306.
45. International Organization for Standardization (ISO) 10993-5:1999. Biological evaluation of medical devices—Part 5: Tests for in vitro cytotoxicity. Available at: www.iso.ch/iso/en/isoonline.frontpage.
46. International Organization for Standardization (ISO) 11979-3:1999. Ophthalmic implants—Intraocular lenses—Part 3: Mechanical properties and test methods. Available at: www.iso.ch/iso/en/isoonline.frontpage.
47. International Organization for Standardization (ISO) 11979-2:1999. Ophthalmic implants—Intraocular lenses—Part 2: Optical properties and test methods. Available at: www.iso.ch/iso/en/isoonline.frontpage.
48. International Organization for Standardization (ISO) 9335:1995. Optics and optical instruments—Optical transfer function—Principles and procedures of measurement. Available at: www.iso.ch/iso/en/isoonline.frontpage.
49. International Organization for Standardization (ISO) 11979-5:1999. Ophthalmic implants—Intraocular lenses—Part 5: Biocompatibility. Available at: www.iso.ch/iso/en/isoonline.frontpage.
50. Koch DD, Samuelson SW, Haft EA, et al. Pupillary size and responsiveness. Implications for selection of a bifocal intraocular lens. *Ophthalmology* 1991;98(7):1030-1035.
51. Hayashi K, Hayashi H, Nakao F, et al. Correlation between pupillary size and intraocular lens decentration and visual acuity of a zonal-progressive multifocal lens and a monofocal lens. *Ophthalmology* 2001;108(11):2011-2017.
52. Crouch ER, Crouch ER Jr, Pressman SH. Prospective analysis of pediatric pseudophakia: myopic shift and postoperative outcomes. *J AAOPS* 2002;6(5):277-282.
53. Plager DA, Kipfer H, Sprunger DT, et al. Refractive change in pediatric pseudophakia: 6-year follow-up. *J Cataract Refract Surg* 2002;28(5):810-815.
54. McClatchey SK, Dahan E, Maselli E, et al. A comparison of the rate of refractive growth in pediatric aphakic and pseudophakic eyes. *Ophthalmology* 2000;107(1):118-122.
55. Roberts C. The cornea is not a piece of plastic. *J Refract Surg* 2000;16(4):407-413.
56. Schwiegerling J, Snyder RW, Lee JH. Wavefront and topography: keratome-induced corneal changes demonstrate that both are needed for custom ablation. *J Refract Surg* 2002;18(5):S584-588.
57. Werner L, Pandey SK, Apple DJ, et al. Anterior capsule opacification: correlation of pathologic findings with clinical sequelae. *Ophthalmology* 2001;108(9):1675-1681.

58. Cochener B, Jacq P-L, Collin J. Capsule contraction after continuous curvilinear capsulorhexis: poly(methyl methacrylate) versus silicone intraocular lenses. *J Cataract Refract Surg* 1999;25(10):1362-1369.
59. Hayashi K, Hayashi H, Nakao F, et al. Reduction in the area of the anterior capsule opening after polymethylmethacrylate, silicone, and soft acrylic intraocular lens implantation. *Am J Ophthalmol* 1997;123(4):441-447.
60. Macky TA, Pandey SK, Werner L, et al. Anterior capsule opacification. *Int Ophthalmol Clin* 2001;41(3):17-31.
61. MacCumber MW, Packo KH, Civantos JM, et al. Preservation of anterior capsule during vitrectomy and lensectomy for retinal detachment with proliferative vitreoretinopathy. *Ophthalmology* 2002;109(2):329-333.
62. Auffarth GU, Schmidbauer J, Becker KA, et al. Miyake-Apple video analysis of movement patterns of an accommodative intraocular lens implant. *Ophthalmologe* 2002;99(11):811-814.
63. Kuchle M, Nguyen NX, Langenbucher A, et al. Two years experience with the new accommodative 1 CU intraocular lens. *Ophthalmologe* 2002;99(11):820-824.